

# Catalysis Science & Technology

Accepted Manuscript



This is an *Accepted Manuscript*, which has been through the Royal Society of Chemistry peer review process and has been accepted for publication.

*Accepted Manuscripts* are published online shortly after acceptance, before technical editing, formatting and proof reading. Using this free service, authors can make their results available to the community, in citable form, before we publish the edited article. We will replace this *Accepted Manuscript* with the edited and formatted *Advance Article* as soon as it is available.

You can find more information about *Accepted Manuscripts* in the [Information for Authors](#).

Please note that technical editing may introduce minor changes to the text and/or graphics, which may alter content. The journal's standard [Terms & Conditions](#) and the [Ethical guidelines](#) still apply. In no event shall the Royal Society of Chemistry be held responsible for any errors or omissions in this *Accepted Manuscript* or any consequences arising from the use of any information it contains.

Revised manuscript for *Cat. Sci & Tech.*  
July 31, 2015

# Theoretical Characterization of First and Second Generation Grubbs Catalysts in Styrene Cross-Metathesis Reactions: Insights From Conceptual DFT

Katherine Paredes-Gil,<sup>a,b\*</sup> Pablo Jaque<sup>a,c</sup>

<sup>a</sup> *Departamento de Ciencias Químicas. Facultad de Ciencias Exactas. Universidad Andres Bello. Av. Republica 275, Santiago, Chile.*

<sup>b</sup> *Departamento de Química, Facultad de Ciencias, Universidad de Chile. Las Palmeras 3425, Santiago, Chile*

<sup>c</sup> *Nucleus Millennium Chemical Processes and Catalysis (CPC), Avenida Vicuña Mackenna 4860, Casilla 306, Correo 22, Santiago, Chile.*

\* *E-mail address:* [katepagi@gmail.com](mailto:katepagi@gmail.com)

**ABSTRACT**

The differences between the first and second generation Grubbs catalysts have been the subject of much interest in olefin metathesis. In this direction, we revised in detail the dissociation reaction of the 16e Grubbs precatalysts and the rotameric change between the 14e inactive to active catalysts using a distortion/interaction model (called here as reorganization energy  $\Delta E_{reorg}$  and interaction energy  $\Delta E_{int}$ ) combined with the DFT-based reactivity descriptors. We have found that there are not great changes between both generations in terms of the interaction energies and electronic descriptors; however, a lower reorganization energy for conformational change in the second generation showed to be significant in agreement with the *reverse trans effect* proposed recently, confirming that structural effects are key role in the reactivity of these Ru-based complexes. Furthermore, the difference of the Grubbs catalysts in the formation of the ruthenacyclobutane intermediate, **RCB** show that the biradical species needed to generate this type of compounds is more easily formed by the second generation than by the first, with  $\Delta E_{reorg\ T-T}(14) = -3.6$  kcal/mol vs 11.8 kcal/mol, respectively. In consequence, the different electronic features of the first and second generation Grubbs catalysts are manifested in the formation of the ruthenacyclobutane intermediates which allow to propose that the higher catalytic activity of the second generation of the Ru-based complexes have also its origin in these effects and not only in structural changes. Finally, we have also found that the dielectric polarizability change showed to be a suitable property to describe the intensity of polarization effects on the formation of ruthenacyclobutane as well as in the identification of the productive and non-productive processes.

## 1. INTRODUCTION

Olefin metathesis has become in routine process in advanced organic synthesis and preparation of new polymeric materials owing to the high versatility in the manipulation of C-C double bonds.<sup>1,2</sup> Molybdenum-based Schrock catalysts together with ruthenium-based complexes, the so-called Grubbs catalysts, are the most important compounds in this field.<sup>3,4,5,6,7</sup> There are two generations of Grubbs precatalysts as displayed Figure 1; while bis-phosphane ruthenium carbene  $[\text{RuCl}_2(=\text{CHPh})(\text{PR}_3)_2]$  complexes belong to the first generation<sup>8</sup> **1a(b)-PC**, the exchange of one  $\text{PR}_3$  ligand by an N-heterocyclic carbene, NHC, generate  $[\text{RuCl}_2(=\text{CHPh})(\text{NHC})(\text{PR}_3)]$  complexes in the second generation **2a(b)-PC**<sup>9,10,11,12</sup> where R = Phenyl or Ph (**a**) and Cyclohexyl or Cy (**b**). Many studies have shown that the second generation catalysts are more efficient than the corresponding phosphane analogous.<sup>13</sup> Originally, it was thought that since the NHC ligand acts as a stronger  $\sigma$ -donor and relatively weaker  $\pi$ -acceptor than  $\text{PR}_3$ , lead to a strong *trans effect* (labilization of the *trans*- $\text{PR}_3$  ligand) in the second generation, which possibly could be responsible for its higher catalytic activity.<sup>14,15</sup> However, taking into account that early mechanism studies recognized to phosphane dissociation as a critical step along the olefin transposition reaction to generate an 14e intermediate which is the catalytically active species that captures an olefinic substrate (see Figure 2); kinetic studies of the phosphane self-exchange reaction revealed, surprisingly, that the exchange in **1b-PC** is relatively faster than in **2b-PC**, the respective rate constants measured at 80 °C are  $9.6 \pm 0.2 \text{ s}^{-1}$  and  $0.13 \pm 0.01 \text{ s}^{-1}$  exhibiting an inverse proportionality with the catalytic activity.<sup>16,17</sup> Furthermore, the activation enthalpy for **1b-PC** and **2b-PC** was reported as  $23.6 \pm 0.5$  and  $27 \pm 2 \text{ kcal/mol}$ , respectively. It must be highlighted that the phosphane self-exchange reactions have been

recently revisited by Nolan and collaborators using  $^{31}\text{P}\{^1\text{H}\}$  EXSY experiments where an excellent agreement was found for **2b-PC** system ( $0.12\text{ s}^{-1}$  and  $27 \pm 7\text{ kcal/mol}$  for rate constant and activation enthalpy, respectively).<sup>18</sup> These data disagree with the original idea and indicate that the Ru-PR<sub>3</sub> bond is stronger in the second than in the first generation Grubbs catalyst by 3.4 kcal/mol. In the light of these results, it was suggested that the rate-limiting step for the second generation is the formation of 14e catalysts, whereas it has not been fully demonstrated for the first generation (see Figure 2). More recently, Torker et al.<sup>19</sup> measured the bond dissociation energy (BDE) in **1b-PC** and **2b-PC** using collision-induced dissociation experiments through electrospray ionization mass spectrometry (ESI-MS); the values of 33.4 and 36.9 kcal/mol, were found, respectively. Again, it can be seen that the Ru-PR<sub>3</sub> bond is stronger in the second generation than in the corresponding phosphane analogous by 3.5 kcal/mol, which agrees with the difference of the activation enthalpies for the phosphane self-exchange reaction.<sup>16,17</sup>

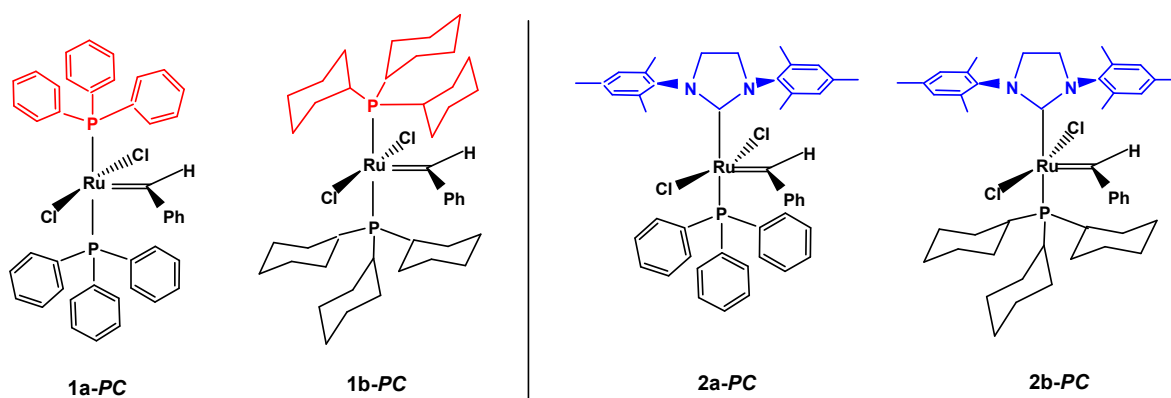


**Figure 1.** First and second generation Grubbs precatalysts **1-2a(b)-PC**.

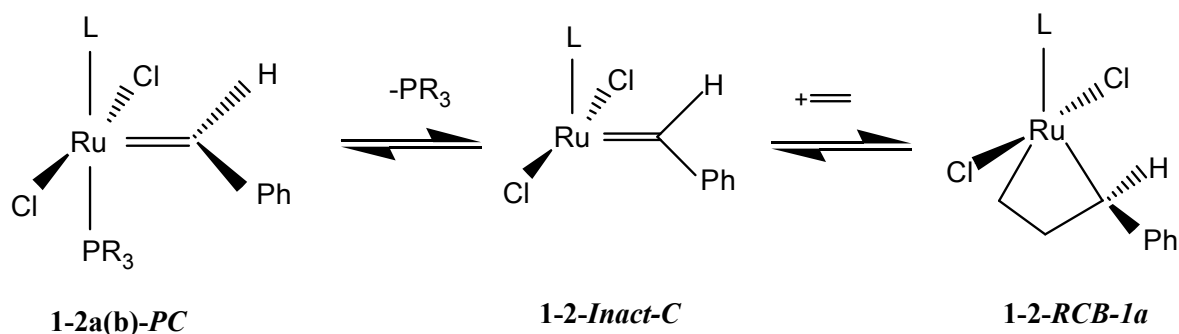


**Figure 2.** Initial stage of the olefin metathesis reaction.

Along with the experimental work, many computational studies have also been reported paying special attention to the *reverse trans effect* introduced by the NHC in the Ru-PR<sub>3</sub> bond dissociation. It is noteworthy that electronic structure of these kind of molecular systems require the treatment of electron correlation for a reliable description as much for bond-breaking process as non-covalent repulsive and attractive interactions due to the presence of bulky ligands such as tricyclohexyl- and triphenyl-phosphane. This makes to Density Functional Theory<sup>20</sup> (DFT) as the more affordable alternative to describe systems displayed in Figures 1-2 owing to its cost-efficiency ratio. An earlier DFT work was reported in 2002 by Cavallo<sup>21</sup> using the exchange-correlation functional BP86 (a GGA-type). This author found that the  $\Delta\text{BDE}(2b-1b)$  agrees reasonably well with those experimental values inferred from the activation enthalpy of **1b-PC** and **2b-PC** reported by Grubbs and co-workers in 2001.<sup>16,17</sup> Later, Tsipis et al.<sup>22</sup> encountered an opposite trend of  $\Delta\text{BDE}$  at both BP86 and B3LYP (a hybrid-GGA-type) levels. This fact was explained on the basis of a new conformer located for the 14e catalysts, which was named as inactive (**2-Inact-C**) and was found to be more stable than the active form (**2-Act-C**), this latter recognized earlier as the most stable in the seminal paper by Cavallo.<sup>21</sup>

On the other hand, in 2007 Zhao and Truhlar<sup>23</sup> reported for first time a good agreement for  $\Delta BDE$  after the discovery by Tsipis and co-workers.<sup>22</sup> This was achieved using the M06L functional (a meta-GGA type), which describes the non-covalent attractive interactions in the electronic structures of the Grubbs precatalysts and catalysts. In a more recent work, Minekov et al.<sup>24</sup> highlighted that dispersion and non-covalent attractive interactions must be taken into account to attain a reliable theoretical description of the geometry and the electronic structure of these types of systems. In this sense, the authors calculated<sup>25</sup> the activation enthalpies, finding excellent agreement with the experimental data. Among many efforts aimed to validate computational protocols in Ru-based catalysts, Poater and co-workers have more recently proposed a highly accurate and cheap procedure (M06/TZVP//BP86/SVP, PCM, P=1,354 atm).<sup>26</sup>

Finally, trying to understand the higher catalytic activity of the second generation, Yang et al.<sup>27</sup> proposed that it might be related to lower rotameric energy between the inactive and active conformers of the 14e catalysts, the energy barrier computed is 4.8 kcal/mol for **2b** vs 13.3 kcal/mol for **1b**. This reveals that carbene rotation acts as a trigger to lead more easily toward the 14e active state in the second generation, **2b-Act-C**, and may be responsible for its reactivity in olefin metathesis.

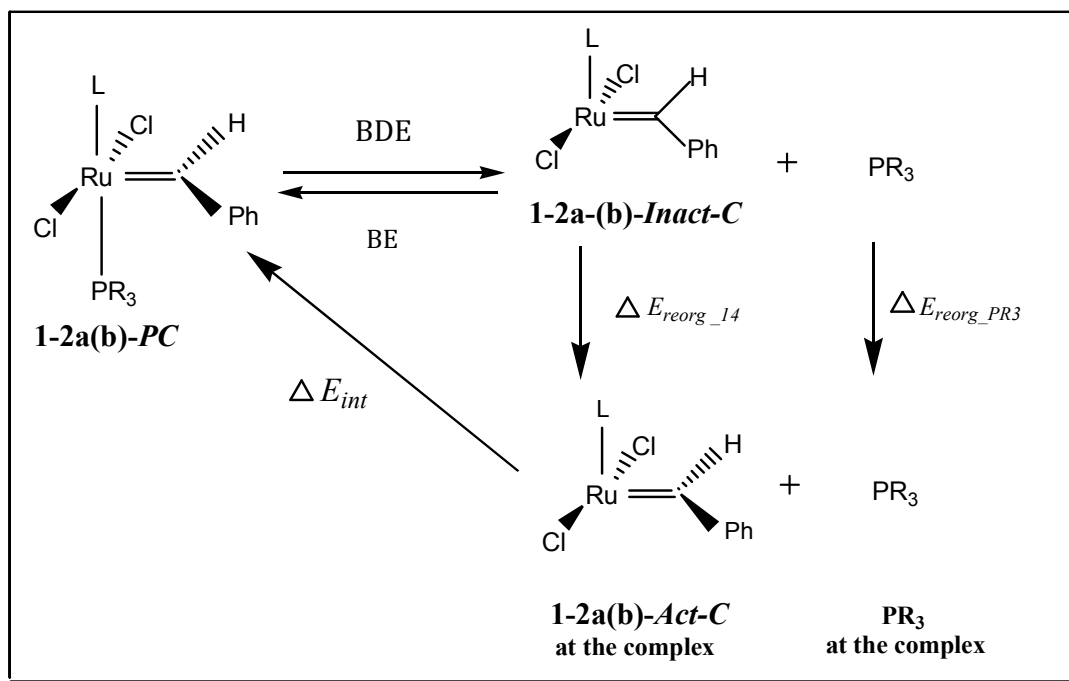
As was pointed out above, the differences between the first and second generation have been a trending topic in olefin metathesis. These studies have been mainly focused in both the dissociation reaction of the 16e precatalysts **1-2a(b)-PC** and the rotameric change between the 14e states **1-2-Inact-C** and **1-2-Act-C** whereas few studies have paid attention

into the differences of the Grubbs catalysts in the formation of the ruthenacyclobutane intermediate, *RCB*, this latter issue is one of the most important at the current work. In spite of intensive theoretical studies, we will revisit in detail the dissociation reaction and the rotameric change from conceptual DFT-based<sup>28</sup> reactivity descriptors (electronic chemical potential  $\mu$ , molecular hardness  $\eta$ , and electrophilicity index  $\omega$ ) viewpoint, which have been successfully applied to characterize a large variety of compounds and reactions such as inorganic compounds<sup>29,30</sup> and homogenous catalysis processes.<sup>31,32</sup> This will be carried out for the styrene cross-metathesis reaction on the basis of an adequate choice of the exchange-correlation functional and basis set for energy and geometry prediction. We expect that this contribution on the reactivity of these important systems will be useful to guide future investigations.

## 2. THEORETICAL BACKGROUND

### 2.1 Computed Ru-PR<sub>3</sub> bond strength in 1-2a(b)-PC

The computed ruthenium-phosphane bond strength ( $BE_{PR_3}$ ) in  $[\text{RuCl}_2(=\text{CHPh})(\text{L})(\text{PR}_3)]$  ( $\text{L}=\text{PR}_3$  or  $\text{NCH}$ ) **1-2a(b)** can be divided into two hypothetical steps displayed in Scheme 1, which is also known as distortion/interaction model by Houk<sup>33</sup> or activation strain model by Bickelhaupt.<sup>34</sup>



**Scheme 1.** Thermodynamic cycle for bond dissociation energy of the  $1-2a(b)-PC$

This thus leads to write the bond strength in terms of the following contributions:<sup>35</sup>

$$BE_{PR_3} = \Delta E_{reorg}(14e) + \Delta E_{reorg}(PR_3) + \Delta E_{int} = -BDE \quad (1)$$

and the interaction energy as

$$\Delta E_{int} = BE_{PR_3} - \Delta E_{reorg} \quad (2)$$

This analysis has been employed in many types of the chemical processes<sup>36,37</sup> and more details can be found in the supporting information. One of current authors has also applied this model to approximate to sulfur-induced copper corrosion through the dibenzyl disulfide adsorption on Cu<sub>7</sub> cluster.<sup>38</sup>

## 2.2 DFT-based reactivity descriptors and Sanderson's principle

Conceptual DFT<sup>28</sup> aims at describing the response of the molecules to perturbations caused by the presence of additional reagent or solvent through the use of chemical reactivity descriptors. In this sense, the electronic chemical potential<sup>39</sup>  $\mu$  and chemical hardness<sup>40</sup>  $\eta$  for an  $N$ -particle system with total energy  $E$  and external potential  $\nu(r)$  are defined as follows:

$$\mu = \left( \frac{\partial E}{\partial N} \right)_{\nu(r)} = -\chi \quad (3)$$

and

$$\eta = \frac{1}{2} \left( \frac{\partial^2 E}{\partial N^2} \right)_{\nu(r)} = \frac{1}{2} \left( \frac{\partial \mu}{\partial N} \right)_{\nu(r)} \quad (4)$$

where  $\mu$  measures the escaping tendency of electrons from the equilibrium and  $\eta$  represents the resistance to charge transfer. The derivatives in Eqs. (3) and (4) can be evaluated using the finite difference approximation. The operational formulas are written in terms of ionization potential  $I$  and electron affinity  $A$  as:  $\mu \approx -\frac{1}{2}(I + A)$  and  $\eta \approx \frac{1}{2}(I - A)$ .

On the other hand, the electrophilicity index<sup>41,42</sup>  $\omega$  is in turn defined as the maximum stabilization of a system when it gains the maximum electron charge from the surroundings, and it is calculated from  $\mu$  and  $\eta$  as:

$$\omega = \frac{\mu^2}{2\eta} \quad (5)$$

Here we are interested in characterizing of the Ru-PR<sub>3</sub> bond formation (or the reverse, i.e. bond dissociation) reaction which can be seen as the resultant of a combination and redistribution of the electron density of the fragments that gives rise to the new composite system. From the rigid fragments can thus be used to introduce some approximations in the calculation of the electronic descriptors of the composite system. It is highlighted that the difference with its value at the complex fully optimized can be rationalized as an effect associated with the relaxation of the electron density as the reaction takes place. In this sense, Sanderson's principle<sup>43</sup> emerges as a suitable alternative to estimate the chemical potential  $\mu_{nf}^o$  of the resultant complex in terms of the chemical potential  $\mu_x^o$  of the  $nf$  rigid fragments  $x$

$$\mu_{nf}^o \approx - \left( \prod_x^{n_f} |\mu_x^o| \right)^{1/n_f} \quad (6)$$

Based on this, Gutiérrez-Oliva and co-workers<sup>44</sup> defined an approach for molecular hardness  $\eta_{nf}^o$  in terms of both  $\mu_x^o$  and  $\eta_x^o$  of different fragments as can be seen in Eq. (7).

$$\eta_{nf}^o = \left( \frac{\partial \mu_{nf}^o}{\partial N} \right)_{v(r)} \approx \frac{\mu_{nf}^o}{n_f} \sum_x^{n_f} \frac{\eta_x^o}{\mu_x^o} \quad (7)$$

From the Sanderson's average for both  $\mu_{nf}^o$  and  $\eta_{nf}^o$  arise a mean for the electrophilicity

$$\text{index as } \omega_{nf}^o = \frac{(\mu_{nf}^o)^2}{2\eta_{nf}^o}.$$

From theoretical viewpoint any relationship between energy and electronic descriptors is valuable since any change in electronic properties can be implying changes in the reaction mechanisms. Accordingly, for each energy contribution associated with the scheme 1 ( $BE_{PR_3}$ ,  $\Delta E_{reorg}$ , and  $\Delta E_{int}$ ) can be defined a variation of the DFT-based reactivity descriptors ( $\Delta\Lambda$ ;  $\Lambda = \mu, \eta, \omega$ ). Thereby, the contribution of the DFT-based reactivity descriptors associated with the overall energy change corresponding to binding energy  $\Delta\Lambda_{BE_{PR_3}}$  is given by the difference between electronic descriptors in the complex and the average of the property related with the reactants. In the current work, we use the Sanderson's average described above,  $\Lambda_{n_f}^o (\mu_{n_f}^o, \eta_{n_f}^o, \omega_{n_f}^o)$ :

$$\Delta\Lambda_{BE_{PR_3}} = \Lambda - \Lambda_{n_f}^o \quad (8)$$

Further, changes of the descriptors associated with the reorganization energy are also defined as:

$$\Delta\Lambda_{reorg} = \Lambda_{14 \text{ and } PR_3 \text{ at the complex}} - \Lambda_{14 \text{ Inact-C and } PR_3}^o \quad (9)$$

And finally, following the eq. 2 the contribution of the chemical potential, hardness and electrophilicity to the interaction energy can be given by:

$$\Delta\Lambda_{int} = \Delta\Lambda_{BE_{PR_3}} - \Delta\Lambda_{reorg} \quad (10)$$

### 2.3 Bond/cycloaddition energy contributions to the formation of the ruthenacyclobutanes

A decomposition analysis for the binding energy between the 14e inactive conformer and olefin to lead the formation of the ruthenacyclobutanes **1a(b)**, **2b-RCB** is described by the thermodynamic cycle depicted in Scheme 2. The overall energy change, i.e.  $BE_{olefin}$ , is

given by Eq. (1) using the respective total energies of all species, i.e.  $E(RCB)$ ,  $E(14e\ Inact - C)$ , and  $E(olefin)$ .

In the decomposition scheme proposed by Poater et al.,<sup>45</sup> the stabilities of **RCB** can be understood in terms of the disappearance of the Ru=C and C=C  $\pi$ -type bonds and the formation of the new Ru-C and C-C  $\sigma$ -type bonds. The disappearance/formation of the  $\pi/\sigma$  bonds occurs through biradical species or triplet states in both species: the 14e catalysts and the olefin. Therefore, the disappearance energy of the Ru=C bond and the C=C  $\pi$  bond, named as  $BDE_{Ru=C}$  and  $BDE_{C=C}$ , is computed from the vertical energy differences between the respective triplet and singlet states at the geometry of the singlet states ( $BDE_{X=C} = E_{X-C}^3 - E_{X-C}^1$ ; X=Ru, C). Thus a triplet-triplet reorganization of the fragments at the relaxed geometry in the ruthenacyclobutane in its ground state takes places, the amount of energy involved in that process is defined as  $\Delta E_{reorg\ T-T}$

$$\begin{aligned} \Delta E_{reorg\ T-T} &= \Delta E_{reorg\ T-T}(14) + \Delta E_{reorg\ T-T}(olefin) \quad (11) \\ &= (E_{14\ at\ the\ complex}^3 - E_{14-Inact-C}^3) + (E_{olefin\ at\ the\ complex}^3 - E_{olefin}^3) \end{aligned}$$

Hence the interaction energy ( $\Delta E_{int}$ ) between the distorted fragments at the triplet states to generate the new Ru-C and C-C  $\sigma$ -type bonds can be computed as indicated by Eq. (12):

$$\Delta E_{int} = BE_{olefin} - (BDE_{Ru=C} + BDE_{C=C} + \Delta E_{reorg\ T-T}) \quad (12)$$



type); PBE0<sup>53</sup> (HGGA-type); and MPWB1K<sup>54</sup> (HMGGA-type). These were combined with a quasi-relativistic pseudopotential developed by Dolg et al.<sup>55</sup>, MWB28, that includes the (8s7p6d)/[6s5p3d] valence basis set to describe the ruthenium atom. The 6-31+G(d,p) basis set<sup>56</sup> was used to describe the carbon, hydrogen, nitrogen, chlorine and phosphorus atoms. For each optimization a vibrational analysis was performed to ensure that the geometries are minima on the potential energy surface. In the prediction of energetic quantities the empirical atom-atom dispersion contributions “D” were taken into account using Grimme's correction<sup>57</sup> as implemented in the AOMIX 6.6 program.<sup>58</sup>

Once the “best” exchange-correlation functional was chosen by comparing the computed data with available experimental data in geometry and BDE, single point energy calculations were performed using a more extended basis set Def2-TZVP<sup>59</sup> to improve the prediction of BDE as well as to compute the input data for  $\mu$  and  $\eta$ , i.e. ionization energy  $I$  and electronic affinity  $A$ .

Finally, to study the differences between the first and the second generation Grubbs catalysts in the formation of the ruthenacyclobutane intermediate, **1a(b)-RCB**, **2b-RCB**, all geometry of the species involved on styrene cross metathesis were optimized followed by vibrational analysis using the “best” exchange-correlation functional (previously selected) together with MWB28/6-31+G(d,p) basis set, single-point energy calculations using Def2-TZVP basis set were also done.

Although the solvent effect are very important in chemical reactivity studies there are not included in the present work owing to our BDE values are compared with data reported by Torker et. al<sup>19</sup> which was measured in gas-phase.

#### 4. RESULTS AND DISCUSSION

The results were divided into the following sections: i) DFT-based methods validation using the experimental geometry and BDE of the 16e precatalysts is presented with the purpose to choose the “best” exchange-correlation functional on the basis of the minima root mean square deviation (RMSD) and unsigned error (UE) for the geometry and BDE, respectively. ii)-iii) the contributions of the bond energy, i.e. reorganization and interaction energies along the Ru-PR<sub>3</sub> bond dissociation in **1-2a(b)-PC** are analyzed as well as the DFT-based reactivity descriptors. iv)-v) Finally, the bond energy contributions involved in the generation of **1a(b)-RCB**, **2b-RCB** intermediates in styrene cross-metathesis reaction are analyzed together with the dielectric polarizability changes ( $\Delta\alpha$ ).

##### 4.1. Performance of DFT-based methods in the prediction of the geometry of Grubbs precatalysts and Ru-phosphane bond dissociation energy.

To evaluate the performance of the DFT-based methods in the prediction of the geometry for 16e precatalysts we took the crystallographic data from the Cambridge Structural Database (CSD) for **2b-PC**, although many others structural information of precatalysts<sup>60,61,62</sup> can be found at the CSD any structural information of those studied by us (**1a(b)- 2a-PC**) are not available. The fully optimized geometries at the local and non-

local DFT-based methods were aligned with the experimental structure using the Quatfit program.<sup>63</sup> The values of RMSD are quoted in Table 1.

**Table 1.** RMSD (in Å) between experimental and fully optimized structures of **2b-PC** using a set of DFT-based methods.

Functional	Type	RMSD
BP86	GGA	0.394
PBE	GGA	0.395
TPSS	MGGA	0.551
M06L	MGGA	0.400
PBE0	HGGA	0.358
MPWB1K	HMGGA	0.442

On the basis of the RMSD values, we noted that the hybrid PBE0 functional is the most accurate reproducing experimental geometry of **2b-PC** in agreement with the study reported by Jiménez-Hoyos et al.<sup>64</sup> who showed that the best geometries for homogeneous catalysts are predicted with range-separated hybrid-GGA functionals. The set of three generically called local (or semi-local) exchange-correlation functionals, BP86, PBE and M06L, deviates by about 40 mÅ from the “best” geometry whereas the largest RMSD were given by the MPWB1K (84 mÅ) and TPSS (193 mÅ) methods. In a detailed study reported by Minenkov and co-workers<sup>24</sup> has been highlighted the performance of the M06L functional in describing geometry of organometallic systems, our results agree with this report even though that it does not present the minimum value of RMSD.

For the assessment of BDE in **1-2(b)-PC** precatalysts DFT-based methods with and without dispersion D corrections were employed. The results are reported in Table 2, they clearly

show that DFT-based methods without dispersion corrections tend to offer poor predictions of BDEs, i.e. Ru-PCy<sub>3</sub> bond in the second generation is predicted much weaker than in the first generation Grubbs precatalysts. Whereas those predicted by using DFT-based methods including dispersion corrections are consistent with the experimental trend. It is noteworthy that the M06L, which accurately describes medium-range correlation energy, and MPWB1K (a HMGGA-type) functionals provide the correct sign of  $\Delta\text{BDE}=\text{BDE}(\mathbf{2b})-\text{BDE}(\mathbf{1b})$  being the M06L closer to the experimental difference of the Ru-PCy<sub>3</sub> bond strength between the second and first generation Grubbs precatalysts. However, the corresponding BDE values are overestimated by around 5.0 kcal/mol.

**Table 2.** Bond Dissociation Energy (BDE) for **1-2b-PC** using a set of DFT-based methods with and without the dispersion “D” corrections. Values are in kcal/mol.

Functional	BDE(1b)	BDE(2b)	$\Delta\text{BDE}(\mathbf{2b-1b})$
BP86	9.5	7.4	-2.1
BP86-D	36.0	38.9	2.9
PBE	14.0	12.7	-1.3
PBE-D	33.2	35.6	2.4
PBE0	22.0	20.6	-1.4
PBE0-D	48.3	52.3	4.0
TPSS	17.3	15.2	-2.1
TPSS-D	42.3	44.9	2.6
M06L	38.5	41.7	3.2
MPWB1K	34.0	36.0	2.0
Exptl.	33.4	36.9	3.5

Basis set: MWB28 (Ru)/6-31+G(d,p) (C, H, N, P, Cl)

By using the M06L functional combined with an extended bases set, e.g. Def2-TZVP, more accurate results are provided. The values of 34.5 and 38.7 kcal/mol are found for BDE of

**1b-PC** and **2b-PC**, respectively. This computational protocol slightly overestimates the Ru-PCy<sub>3</sub> bond strength by an amount less than 2.0 kcal/mol. The prediction of the BDE of Ru-tricyclophenyl phosphane in the 16e precatalysts using M06L/Def2-TZVP level is 24.8 and 29.1 kcal/mol for **1a-PC** and **2a-PC**, respectively. Concomitantly, all energy contributions along this work were computed at the M06L/Def2-TZVP level of theory.

One issue that deserves to be highlighted on the reliability of our results with respect to some early predictions<sup>23,65,66</sup> of BDE is the fact that they employed the “*pseudo-E*” conformational isomer of the precatalysts **2b-PC** in their calculations, which is higher in energy than the corresponding X-ray crystallographic structure, called “*pseudo-Z*” isomer (Figure S1, Supporting Information) by a range of 4.0-5.0 kcal/mol at the set of DFT-based levels used by us (see Table S1 in Supporting Information).

#### 4.2. Ru-phosphane bond energy contributions in 1-2a(b)-PC: $\Delta E_{reorg}$ and $\Delta E_{int}$

The Ru-phosphane bond energy ( $BE_{PR_3}$ ), reorganization ( $\Delta E_{reorg}$ ), and interaction ( $\Delta E_{int}$ ) were calculated for the precatalysts **1-2a(b)-PC**. The results are collected in Table 3.

**Table 3.**  $\Delta E_{reorg}$  and  $\Delta E_{int}$  for **1-2a(b)-PC**. Values are in kcal/mol.

<i>PC</i>	BDE	$\Delta E_{reorg}$ 14	$\Delta E_{reorg}$ PR <sub>3</sub>	$\Delta E_{int}$
<b>1a</b>	24.8	16.4	2.1	-43.3
<b>2a</b>	29.1	13.0	0.8	-42.9
<b>1b</b>	34.5	20.8	1.8	-57.1
<b>2b</b>	38.7	14.4	2.6	-55.7

These show two important features:  $\Delta E_{reorg}$  14 can be seen as the rotameric change from the 14e inactive (**1-2a(b)-Inact-C**) towards the active (**1-2a(b)-Act-C**) state, as it is displayed in Scheme 1. The energy difference between the first and second generation Grubbs catalysts is  $\Delta\Delta E_{reorg}$  14 (**2-1**) = -3.4 and -6.4 kcal/mol when R is Ph (**a**) and Cy (**b**), respectively. Which qualitatively agrees with the rotameric energy reported by Yang and co-workers<sup>27</sup>:  $\Delta\Delta E_{rotameric}$  (**2b-1b**) = -8.5 kcal/mol. Consequently, the higher catalytic activity of the second generation Grubbs catalyst can thus be related to a lower structural reorganization required to lead to the **2a(b)-Act-C** conformer, which turns into the species that capture the olefin and promote toward the next steps along the catalytic cycle. The second important aspect is referred to the interaction energy,  $\Delta E_{int}$ , which reveals how much strong is the interaction and bonding between the distorted fragments. This contribution showed to be higher than that associated with the structural reorganization  $\Delta E_{reorg}$  to the Ru-PR<sub>3</sub> bond strength in any studied system here. As can be seen the second generation **2a(b)-PC** presents very slightly lower interaction energy than the first by about of 0.4 (1.4) kcal/mol for  $\Delta\Delta E_{int}$ , supporting the idea that the interaction and bonding is quite similar in both generations, concomitantly, the effect by functionalizing the precatalysts from phosphane to NHC induces only a minor perturbation into the molecules as already was pointed out by Getty and co-workers.<sup>67</sup> Therefore, these properties play a key role in the reactivity of the Grubbs catalysts, as we have recently reported in a previous study.<sup>68</sup>

### 4.3. Rationalization of Ru-phosphane bond dissociation energies for **1-2a(b)-PC** through the use of DFT-based reactivity descriptors.

To gain insights on the Ru-phosphane bond dissociation process in **1-2a(b)-PC**, we analyzed how the DFT-based descriptors change once the dissociation process takes place. For this purpose we have taken such variations in the way of dissociation as:  $\Delta\Lambda_{BDEPR_3} = \Lambda_{nf}^o - \Lambda_{PC}$ ;  $\Lambda = \mu, \eta, \omega$ . Their values are quoted in Table 4. It can be noted that the chemical potential change  $\Delta\mu$  depends on the nature of the phosphane ligand, the Sanderson's value  $\mu_2^o$  of the isolated fragments is higher than the respective value of the complex for **1-2b-PC**, while the reverse is noted for **1-2a-PC**. By following the direction of a spontaneous way, i.e. from higher  $\mu$  value to lower  $\mu$  value, it thus drives the formation of the 16e precatalysts in **1-2b-PC** whereas towards the generation of isolated fragments, i.e. the 14e catalysts and triphenylphosphane, in **1-2a-PC**. Nevertheless, the difference of  $\Delta\mu$  between the second and first Grubbs generation catalysts is lower than 2 kcal/mol, showing, again, that the alteration from phosphane to NHC ligand results in minor deviation of the overall interactions or bonding in the molecules.

**Table 4.** BDE and variation of the DFT-reactivity descriptors. ( $\Delta\Lambda_{BDEPR_3}$ ,  $\Lambda = \mu, \eta, \omega$ ).

Values are in kcal/mol.

PC/ $\Delta\Lambda_{BDEPR_3}$	BDE	$\Delta\mu$	$\Delta\eta$	$\Delta\omega$
<b>1a</b>	24.8	-2.5	18.6	-11.1
<b>2a</b>	29.1	-3.4	20.4	-10.7
<b>1b</b>	34.5	7.2	36.4	-26.9
<b>2b</b>	38.7	5.8	34.9	-23.7

It is also noticed that the molecular hardness change,  $\Delta\eta$ , is higher than the chemical potential change although there are only slight variations from one Grubbs generation to the next by almost 2 kcal/mol plausibly due to the fact that the overall bonding in both types of complexes is quite similar. The values show that the isolated fragments are harder species than the composite systems being more significant in **1-2b-PC**. This is in agreement with the experimental evidences on the higher activity of **1-2b-PC** than **1-2a-PC**. Electrophilicity index is a DFT-based descriptor that brings both  $\mu$  and  $\eta$  and it has been proposed as a kinetic descriptor.<sup>69</sup> The negative values of  $\Delta\omega$  are indicative that the 16e complexes are much better electrophile than the respective isolated fragments, this quality is more important in **1a(b)-PC** than in **2a(b)-PC** by 0.4 (3.2) kcal/mol, respectively. Taking into account the fact that the first Grubbs generation is more electrophile species than the second category, this opposes to the dissociation pathway and consequently the second generation complexes are more reactive than the first.

On the other hand, the DFT-based reactivity descriptors changes associated with  $\Delta E_{reorg}$  and  $\Delta E_{int}$  have a similar tendency to that above-mentioned for BDE. The values are tabulated in Tables S2 and S3 of the Supporting Information. The results show, for instance, that the second generation presents a slightly charge transfer change when **2-Inact-C** goes to **2-Act-C** plausibly due to that fact this process is driven by electron delocalization factors as was concluded in a recent article reported by us.<sup>68</sup> Such behavior produces an electrophilicity index change  $\Delta\omega(2-1) = -8.8$  kcal/mol. Which agrees with the value reported by Yang and co-workers<sup>27</sup> for the rotameric energy suggesting, thus, that the origin of the rotameric change is driven rather by electronic factors than structural factors, owing to the differences in the nature of ligand L ( $PR_3$  vs NHC). Moreover, the analysis of

the DFT-based reactivity descriptors to the interaction energy again showed only slight difference between both generations in agreement with the fact that the overall bonding and interaction into the molecules are quite similar in the substitution of phosphane by NHC ligand.

#### 4.4. $BDE_{Ru=C}$ , $BDE_{C=C}$ , $\Delta E_{reorg\ T-T}$ , and $\Delta E_{int}$ terms involved in the formation of ruthenacyclobutanes (1a(b), 2b-RCB) in styrene cross-metathesis reaction

A complete description of the styrene cross-metathesis reaction involves a total of 13 processes which originate around two types of 14e inactive catalysts  $L-Cl_2Ru=CH_2$  and  $L-Cl_2Ru=CHPh$  ( $L=PR_3, NHC$ ), and four olefins: ethene, styrene, and *cis*- and *trans*-stilbene, as we have reported previously.<sup>70,71</sup> Ten different ruthenacyclobutanes are potentially obtained in the reaction mixture, and they are depicted in Figure 3.

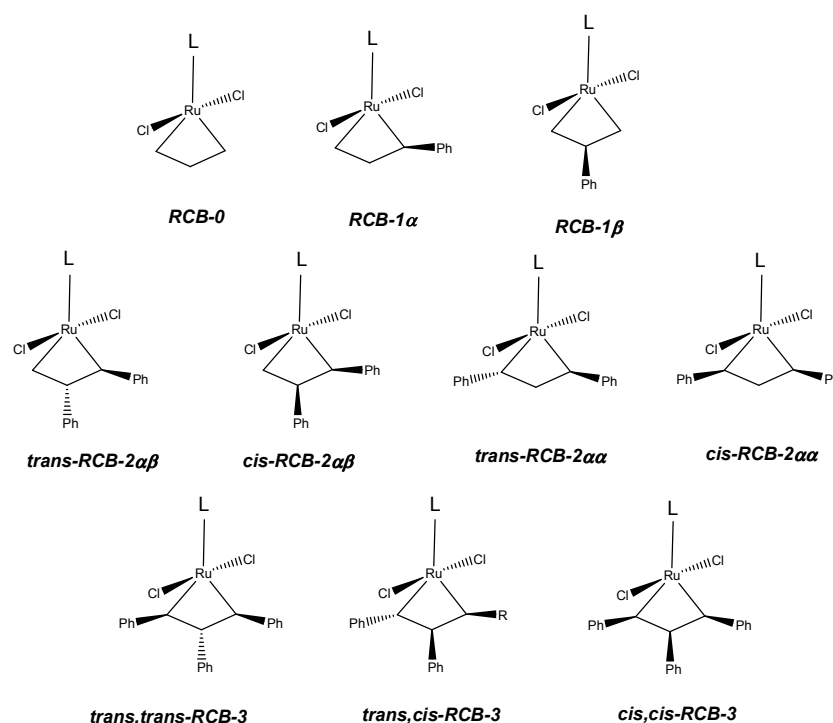


**Figure 3.** Ruthenacyclobutanes (1a-b, 2b-RCB) involved in styrene cross-metathesis reaction.

On the other hand, the bond energy ( $BE_{olefin}$ ) of all ten ruthenacyclobutanes and their energy contributions ( $\Delta E_{reorg\ T-T}$ ,  $\Delta E_{int}$ ) are quoted in Tables 5 and 6 for **1b-RCB** and **2b-RCB**, respectively, while values for **1a-RCB** are reported in Table S4 of the Supporting Information. The  $BE_{olefin}$  shows that the second generation form more stable ruthenacyclobutanes than the first generation Grubbs catalysts. In both **RCB-0** is the most stable ruthenacyclobutanes, followed by **RCB-1 $\alpha$** , while the di- and tri-substituted ruthenacyclobutanes **RCB-2 $\alpha\beta$**  and **RCB-3** are less stable even these are unstable for **1b-RCB**. Specifically, the  $BE_{olefin}$  values of the first generation are between -13.6 and 9.3 kcal/mol, while for the second generation they are between -25.5 and -6.8 kcal/mol. It must be pointed out that, there are very few theoretical studies of the  $BE_{olefin}$  of ruthenacyclobutanes. Recently, Minenkov et al. reported  $BE_{olefin}$  associated with the coordination of norbornene by the second generation Grubbs catalyst as -33.4 kcal/mol.<sup>72</sup>

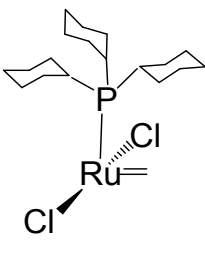
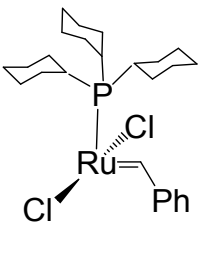
The values calculated by the disappearance of the Ru=C and C=C  $\pi$ -type bonds,  $BDE_{Ru=C}$  and  $BDE_{C=C}$ , are collected in Table 7. Notice that the values of  $BDE_{C=C}$  to different olefins are higher than the values for the  $BDE_{Ru=C}$ , showing that the former involve more energy than the conversion of the Ru=C  $\pi$ -type bond into Ru-C  $\sigma$ -type bond in the 14e inactive catalysts. As can be seen the increase of the substituents on the olefins as well as the spatial arrangement of them decrease the  $BDE_{C=C}$ , which is related to the stabilization of the triplet state assisting the subsequent reorganization. On the other hand, while there is no energy changes in the first generation Grubbs catalysts when in Ru=CHR R=H is replaced by R=Ph, it is observed that L-Cl<sub>2</sub>Ru=CH<sub>2</sub> has 8.5 kcal/mol less than L-Cl<sub>2</sub>Ru=CHPh. In

consequence, the presence of a bulky substituent hinders the change of the Ru=C  $\pi$ -type bond into a Ru-C  $\sigma$ -type bond in the 14e second generation catalytic species.

It is important to pay attention on the stabilization of the ruthenacyclobutanes that is mainly due to the formation of Ru-C and C-C  $\sigma$ -type bonds and thus described by the term  $\Delta E_{int}$ . This energy is close to -140.0 kcal/mol for unsubstituted ruthenacyclobutanes and -100.0 kcal/mol for trisubstituted ruthenacyclobutanes. As can be also noticed that the  $\Delta E_{reorg T-T}$  (14) for **1b-RCB** is between 0.8 and 18.2 kcal/mol, while for **2b-RCB** from NHC-Cl<sub>2</sub>Ru=CH<sub>2</sub> is in the range of 4.0 and 7.3 kcal/mol, and between -0.4 and -5.4 kcal/mol for NHC-Cl<sub>2</sub>Ru=CHPh. This indicates that while the triplet-triplet reorganization involves the 14e inactive **14e-Inact-C** conformer into the ruthenacyclobutanes as the most stable species in the first generation, while it is the **14e-Act-C** in the second generation. These results show that the biradical species needed to produce the ruthenacyclobutanes are easily created by the second generation whereas it is not possible by the first generation Grubbs catalysts (e.g. in the case of **2b-RCB-1 $\alpha$**  vs **1b-RCB-1 $\alpha$**  we got a value of  $\Delta\Delta E_{reorg T-T}$  equal to -15.4 kcal/mol). Therefore,  $\Delta E_{reorg T-T}$  (14) can be providing a key property to understand the highest catalytic activity of the second generation. Finally, it is also seen that the lowest values of  $\Delta E_{reorg T-T}$  (14) correspond to the *trans*- and *cis*-**RCB-2 $\alpha\beta$** , which are intermediates that will bring into being the *trans*- and *cis*-stilbene, showing a direct relation with the *Z/E* selectivity of the cross metathesis reaction and reinforcing the fact that its energetic has a determining role into the global reactivity of the second generation.

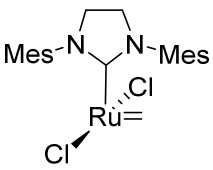
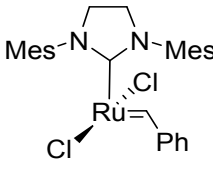
**Table 5.**  $BE_{olefin}$ ,  $\Delta E_{reorg T-T}(14)$ , and  $\Delta E_{int}$  for the ruthenacyclobutanes **1b-RCB**.

Values are in kcal/mol.

Reactants		<b>1b-RCB</b>	$BE_{olefin}$	$\Delta E_{reorg T-T}(14)$	$\Delta E_{int}$
	+ ethene	<b>RCB-0</b>	-13.6	0.9	-137.5
	+ styrene	<b>RCB-1<math>\alpha</math></b>	-12.2	10.6	-137.0
	+ styrene	<b>RCB-1<math>\beta</math></b>	-3.8	1.6	-133.5
	+ <i>cis</i> -stilbene	<b><i>cis</i>-RCB-2<math>\alpha\beta</math></b>	-6.9	6.4	-133.4
	+ <i>trans</i> -stilbene	<b><i>trans</i>-RCB-2<math>\alpha\beta</math></b>	-2.0	10.9	-131.2
	+ ethene	<b>RCB-1<math>\alpha</math></b>	-2.4	11.8	-134.2
	+ styrene	<b><i>trans</i>-RCB-2<math>\alpha\alpha</math></b>	1.4	18.7	-131.7
	+ styrene	<b><i>cis</i>-RCB-2<math>\alpha\alpha</math></b>	0.8	10.3	-123.9
	+ styrene	<b><i>trans</i>-RCB-2<math>\alpha\beta</math></b>	7.1	14.2	-123.3
	+ styrene	<b><i>cis</i>-RCB-2<math>\alpha\beta</math></b>	9.3	14.3	-124.2
	+ <i>trans</i> -stilbene	<b><i>trans,trans</i>-RCB-3</b>	-0.4	7.5	-120.9
	+ <i>trans</i> -stilbene	<b><i>trans,cis</i>-RCB-3</b>	2.6	2.2	-109.2
	+ <i>cis</i> -stilbene	<b><i>cis,cis</i>-RCB-3</b>	1.9	5.1	-123.3

**Table 6.**  $BE_{olefin}$ ,  $\Delta E_{reorg\ T-T}(14)$ , and  $\Delta E_{int}$  for the ruthenacyclobutanes **2b-RCB**.

Values are in kcal/mol.

Reactants		<b>2b-RCB</b>	$BE_{olefin}$	$\Delta E_{reorg\ T-T}(14)$	$\Delta E_{int}$
	+ ethene	<b>RCB-0</b>	-25.5	4.0	-148.8
	+ styrene	<b>RCB-1<math>\alpha</math></b>	-24.4	5.4	-140.7
	+ styrene	<b>RCB-1<math>\beta</math></b>	-16.4	5.3	-141.6
	+ <i>cis-stilbene</i>	<b><i>cis</i>-RCB-2<math>\alpha\beta</math></b>	-21.3	7.3	-147.8
	+ <i>trans-stilbene</i>	<b><i>trans</i>-RCB-2<math>\alpha\beta</math></b>	-15.9	6.1	-137.0
	+ ethene	<b>RCB-1<math>\alpha</math></b>	-19.0	-3.6	-142.2
	+ styrene	<b><i>trans</i>-RCB-2<math>\alpha\alpha</math></b>	-14.4	-1.4	-135.9
	+ styrene	<b><i>cis</i>-RCB-2<math>\alpha\alpha</math></b>	-17.5	-0.4	-136.0
	+ styrene	<b><i>trans</i>-RCB-2<math>\alpha\beta</math></b>	-11.2	-4.5	-127.8
	+ styrene	<b><i>cis</i>-RCB-2<math>\alpha\beta</math></b>	-9.5	-5.4	-124.6
	+ <i>trans-stilbene</i>	<b><i>trans,trans</i>-RCB-3</b>	-9.4	-0.4	-128.3
	+ <i>trans-stilbene</i>	<b><i>trans,cis</i>-RCB-3</b>	-6.8	-4.2	-117.4
	+ <i>cis-stilbene</i>	<b><i>cis,cis</i>-RCB-3</b>	-8.1	-1.4	-129.4

**Table 7.** BDE<sub>C=C</sub> and BDE<sub>Ru=C</sub> as a contribution to the  $BE_{olefin}$  of the **1a-b, 2b-RCB**.

Values are in kcal/mol.

olefin	BDE <sub>C=C</sub>	RCB	BDE <sub>Ru=C</sub>	BDE <sub>Ru=C</sub>
			L-Cl <sub>2</sub> Ru=CH <sub>2</sub>	L-Cl <sub>2</sub> Ru=CHPh
ethene	99.1	<b>1a</b>	33.4	33.4
styrene	72.6	<b>1b</b>	36.0	35.8
<i>cis</i> -stilbene	72.4	<b>2b</b>	32.1	40.6
<i>trans</i> -stilbene	56.4			

#### 4.5. Polarizability changes and $BE_{olefin}$ of the ruthenacyclobutanes (**1a(b), 2b-RCB**) involved in styrene cross-metathesis reaction.

By taking into account that the **RCB** are dominated by polarization effects,<sup>68,73</sup> we studied the polarizability change  $\Delta\alpha$  associated with the formation of all the ruthenacyclobutanes involved in styrene cross-metathesis.  $\alpha$  can be seen as the response of a molecular systems in the presence of a static electric field. Thus  $\Delta\alpha$  associated with the formation of ruthenacyclobutanes is given by:

$$\Delta\alpha = \alpha(RCB) - [\alpha(14e\ Inact - C) + \alpha(olefin)] \quad (13)$$

We have found that  $\Delta\alpha$  for the 13 processes involved in styrene cross-metathesis can be divided into two main groups as can be seen in Figure 4. The first group corresponds to the reaction set with a significant reduction of dielectric polarizability according to the formation of ruthenacyclobutanes take place ( $\Delta\alpha \approx -100$  to  $-80 a_0^3$ ), while the second is related to lower values ( $\Delta\alpha \approx -20$  to  $20 a_0^3$ ). Noticed that the former corresponds to the formation of tri- and disubstituted ruthenacyclobutanes **RCB-3** and **RCB-2 $\alpha\beta$** , while the second group involves the unsubstituted and monosubstituted ruthenacyclobutanes **RCB-0**

and **RCB-1 $\alpha$**  which are, respectively, less and more stable intermediates. These results indicate that ruthenacyclobutanes with highly reduced polarizability change will produce the *trans*- and *cis*-stilbenes connected with non-productive processes, while minor  $\Delta\alpha$  are associated with the formation of **RCB** that lead to productive processes in the cross-metathesis reaction. Therefore, the formation of **RCB** associated with productive (non-productive) processes are characterized by small (negative)  $\Delta\alpha$  values suggesting that the former are stabilized by increasing dispersion forces while in the latter those forces become weaker.

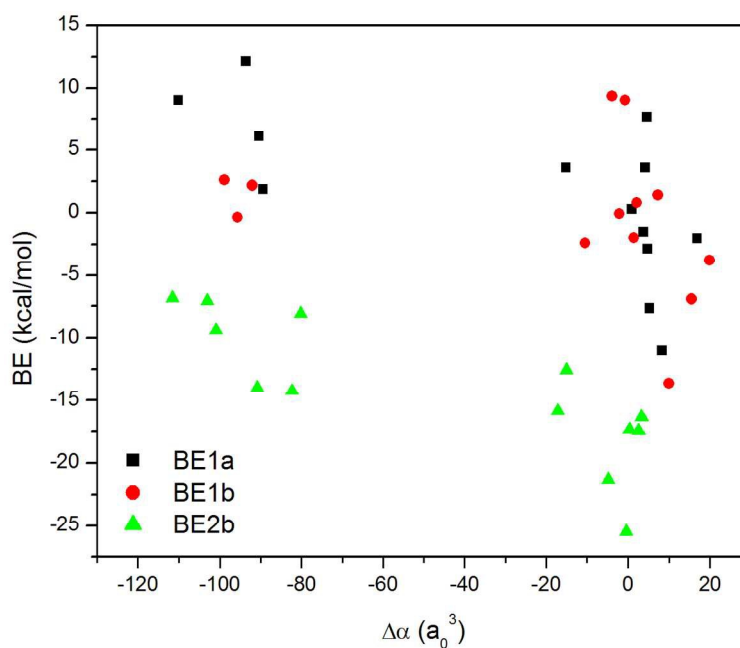


**Figure 4.**  $BE_{olefin}$  vs.  $\Delta\alpha$  for all ruthenacyclobutanes (**RCB**) involved in the styrene cross-metathesis reaction.

## CONCLUSIONS

In the theoretical characterization of the first and second generation Grubbs catalysts in styrene cross-metathesis reactions we have found that the donor-acceptor properties of the NHC ligand not exert an important role in the dissociation of the Ru-PR<sub>3</sub> bond in the 16e precatalysts. Also, the rotameric interconversion between **1a(b)**, **2-Inact-C** and **1a(b)**, **2-Act-C** states is mainly characterized by a structural reorganization, but electronic aspects related to the nature of the ligand L also play an important role in the low rotameric energy observed in the second generation Grubbs catalysts. Finally, the differences between the first and second generation in the formation of the ruthenacyclobutane, **RCB**, were also explored. Employing the second generation than the first more easily generates the biradical species needed to obtain the respective **RCB** compounds, this was associated with the low value of  $\Delta E_{reorg\ T-T}(14)$ . Therefore, the higher catalytic activity of the second generation has its origin in the electronic changes of the initial stage and it is not uniquely due to the lower energy barrier for the interconversion between **2-Inact-C** and **2-Act-C** conformers as was recently reported.

## ACKNOWLEDGEMENTS:

The authors acknowledge the support of FONDECYT through project 1140340 and 1140503, the project CONICYT AKA ERNC-001 and Millenium Nucleus CPC Grant NC120082. K. P.-G. acknowledges UNAB-DI-08-11/I Grant and a MECESUP fellowship.

**SUPPORTING INFORMATION:**

Table S1 reports the energy difference between *E*- and *Z*-**2b-PC**. Tables S2 and S3 contain the energy contributions  $\Delta E_{reorg}$  and  $\Delta E_{int}$ , in terms of the DFT-reactivity descriptors, respectively. Table S4 shows the  $BE_{olefin}$ ,  $\Delta E_{reorgT-T}(14)$ , and  $\Delta E_{int}$  for the ruthenacyclobutanes **1a-RCB**. A complete list of all the computed molecules and their Cartesian coordinates are added.

**REFERENCES**

- 1 E. Grau and S. Mecking, *Green Chem.*, 2013, **15**, 1112-1116.
- 2 M. Wathier, B. a Lakin, P. N. Bansal, S. S. Stoddart, B. D. Snyder and M. W. Grinstaff, *J. Am. Chem. Soc.*, 2013, 36-39.
- 3 R. R. Schrock, J. S. Murdzek, G. C. Bazan, J. Robbins, M. DiMare and M. O'Regan, *J. Am. Chem. Soc.*, 1990, **112**, 3875-3886.
- 4 R. R. Schrock and A. H. Hoveyda, *Angew. Chem. Int. Ed. Engl.*, 2003, **42**, 4592-4633.
- 5 R. R. Schrock, *Angew. Chem. Int. Ed. Engl.*, 2006, **45**, 3748-3759.
- 6 S. T. Nguyen, L. K. Johnson, R. H. Grubbs and J. W. Ziller, *J. Am. Chem. Soc.*, 1992, **114**, 3974-3975.
- 7 R. H. Grubbs, *Angew. Chem. Int. Ed. Engl.*, 2006, **45**, 3760-3765.
- 8 P. Schwab, R. H. Grubbs, J. W. Ziller and R. V August, *J. Am. Chem. Soc.*, 1996, **118**, 100-110.
- 9 M. Scholl, S. Ding, C. W. Lee and R. H. Grubbs, *Org. Lett.*, 1999, **1**, 953-956.
- 10 M. S. Sanford, J. A. Love and R. H. Grubbs, *Organometallics*, 2001, 5314-5318.
- 11 J. Huang, E. D. Stevens, S. P. Nolan, J. L. Petersen, N. Orleans, W. Virginia, V. Uni and R. V September, *J. Am. Chem. Soc.*, 1999, **121**, 2674-2678.

- 12 J. Huang, H.-J. Schanz, E. D. Stevens and S. P. Nolan, *Organometallics*, 1999, **18**, 5375–5380.
- 13 E. L. Dias, S. T. Nguyen and R. H. Grubbs, *J. Am. Chem. Soc.*, 1997, **119**, 3887–3897.
- 14 H. Jacobsen, A. Correa, C. Costabile and L. Cavallo, *J. Organomet. Chem.*, 2006, **691**, 4350–4358.
- 15 N. S. Antonova, J. J. Carbó and J. M. Poblet, *Organometallics*, 2009, **28**, 4283–4287.
- 16 M. S. Sanford, J. A. Love and R. H. Grubbs, *J. Am. Chem. Soc.*, 2001, **123**, 6543–6554.
- 17 M. S. Sanford, M. Ulman and R. H. Grubbs, *J. Am. Chem. Soc.*, 2001, **123**, 749–750.
- 18 A. Urbina-blanco, A. Poater, T. Lebl, S. Manzini, A. M. Z. Slawin, L. Cavallo and S. P. Nolan, *J. Am. Chem. Soc.*, 2013, **135**, 7073–7079.
- 19 S. Torker, D. Merki and P. Chen, *J. Am. Chem. Soc.*, 2008, **130**, 4808–4814.
- 20 R. Parr and W. Yang, *Density functional theory of atoms and molecules*, 1989.1-338
- 21 L. Cavallo, *J. Am. Chem. Soc.*, 2002, **124**, 8965–8973.
- 22 A. C. Tsipis, a G. Orpen and J. N. Harvey, *Dalton Trans.*, 2005, 2849–2858.
- 23 Y. Zhao and D. G. Truhlar, *Org. Lett.*, 2007, **9**, 1967–1970.
- 24 Y. Minenkov, A. Singstad, G. Occhipinti and V. R. Jensen, *Dalton Trans.*, 2012, **41**, 5526–5541.
- 25 Y. Minenkov, G. Occhipinti, W. Heyndrickx and V. R. Jensen, *Eur. J. Inorg. Chem.*, 2012, **2012**, 1507–1516.
- 26 A. Poater, E. Pump, S. Vummaleti and L. Cavallo, *J. Chem. Theory Comput.*, 2014, **10**, 4442–4448.
- 27 H.-C. Yang, Y.-C. Huang, Y.-K. Lan, T.-Y. Luh, Y. Zhao and D. G. Truhlar, *Organometallics*, 2011, **30**, 4196–4200.
- 28 P. Geerlings, F. De Proft and W. Langenaeker, *Chem. Rev.*, 2003, **103**, 1793–1873.
- 29 P. Jaque and A. Toro-Labbé, *J. Chem. Phys.*, 2002, **117**, 3208–3218.

- 30 A. Poater, M. Duran, P. Jaque, A. Toro-Labbé and M. Solà, *J. Phys. Chem. B*, 2006, **110**, 6526–6536.
- 31 J. Ignacio Martínez-Araya, R. Quijada and A. Toro-Labbé, *J. Phys. Chem.*, 2012, **116**, 21318–21325.
- 32 J. Martínez, V. Cruz, J. Ramos, S. Gutiérrez-Oliva, J. Martínez-Salazar and A. Toro-Labbé, *J. Phys. Chem.*, 2008, **112**, 5023–5028.
- 33 D. H. Ess and K. N. Houk, *J. Am. Chem. Soc.*, 2007, **129**, 10646–10647.
- 34 F. Bickelhaupt, *J. Comput. Chem.*, 1999, **20**, 114–128.
- 35 J.-Z. Ramírez-Ramírez, R. Vargas, J. Garza and J. L. Gázquez, *J. Phys. Chem. A*, 2010, **114**, 7945–7951.
- 36 A. G. Green, P. Liu, C. a Merlic and K. N. Houk, *J. Am. Chem. Soc.*, 2014, **136**, 4575–4583.
- 37 K. M. Engle, G. Lu, S.-X. Luo, L. M. Henling, M. K. Takase, P. Liu, K. N. Houk and R. H. Grubbs, *J. Am. Chem. Soc.*, 2015, **137**, 5782–5792.
- 38 M. Saavedra-Torres, P. Jaque, F. Tielens and J. C. Santos, *Theor. Chem. Acc.*, 2015, **134**, 73–82.
- 39 R. G. Pearson, *J. Am. Chem. Soc.*, 1989, 1423–1430.
- 40 R. G. Parr and R. G. Pearson, *J. Am. Chem. Soc.*, 1983, **105**, 7512–7516.
- 41 R. G. Parr, L. v. Szentpaly and S. Liu, *J. Phys. Chem.*, 1999, **121**, 1922–1924.
- 42 P. K. Chattaraj, U. Sarkar and D. R. Roy, *Chem. Rev.*, 2011, **111**, PR43–PR74.
- 43 R. G. Parr and L. J. Bartolotti, *J. Am. Chem. Soc.*, 1982, **3680**, 3801–3803.
- 44 S. Gutiérrez-Oliva, P. Jaque and A. Toro-Labbé, *J. Phys. Chem. A*, 2000, **104**, 8955–8964.
- 45 A. Poater, X. Solans-Monfort, E. Clot, C. Copéret, O. Eisenstein. *J. Am. Chem. Soc.*, 2007, **129**, 8207–8216.
- 46 J. R. . Frisch, M. J.; Trucks, G. W.; Schlegel, H. B.; Scuseria, G. E.; Robb, M. A.; Cheeseman, S. S. . Montgomery, Jr., J. A.; Vreven, T.; Kudin, K. N.; Burant, J. C.; Millam, J. M.; Iyengar, G. A. . Tomasi, J.; Barone, V.; Mennucci, B.; Cossi, M.; Scalmani, G.; Rega, N.; Petersson, M. . N. Nakatsuji, H.; Hada, M.; Ehara, M.; Toyota, K.; Fukuda, R.; Hasegawa, J.; Ishida, J. B. . T.; Honda, Y.; Kitao, O.; Nakai,

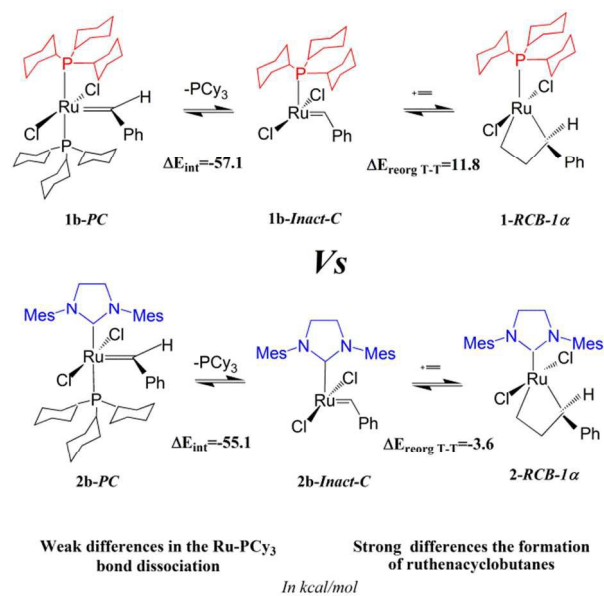
- H.; Klene, M.; Li, X.; Knox, J. E.; Hratchian, H. P.; Cross, A. J. . Bakken, V.; Adamo, C.; Jaramillo, J.; Gomperts, R.; Stratmann, R. E.; Yazyev, O.; Austin, P. . Cammi, R.; Pomelli, C.; Ochterski, J. W.; Ayala, P. Y.; Morokuma, K.; Voth, G. A.; Salvador, O. . Dannenberg, J. J.; Zakrzewski, V. G.; Dapprich, S.; Daniels, A. D.; Strain, M. C.; Farkas, Q. . B. Malick, D. K.; Rabuck, A. D.; Raghavachari, K.; Foresman, J. B.; Ortiz, J. V.; Cui, P. . A. G.; Clifford, S.; Cioslowski, J.; Stefanov, B. B.; Liu, G.; Liashenko, A.; Piskorz, C. Y. . N. Komaromi, I.; Martin, R. L.; Fox, D. J.; Keith, T.; Al-Laham, M. A.; Peng, C. . P. A.; Challacombe, M.; Gill, P. M. W.; Johnson, B.; Chen, W.; Wong, M. W.; Gonzalez and J. A., 2003.
- 47 G. E. . Frisch, M. J.; Trucks, G. W.; Schlegel, H. B.; Scuseria, V. . M. Robb, M. A.; Cheeseman, J. R.; Scalmani, G.; Barone, H. B.; Petersson, G. A.; Nakatsuji, H.; Caricato, M.; Li, X.; Hratchian, M. . P.; Izmaylov, A. F.; Bloino, J.; Zheng, G.; Sonnenberg, J. L.; Hada, M. . N. Ehara, M.; Toyota, K.; Fukuda, R.; Hasegawa, J.; Ishida, J. . T.; Honda, Y.; Kitao, O.; Nakai, H.; Vreven, T.; Montgomery, J. A., E. . K. Peralta, J. E.; Ogliaro, F.; Bearpark, M.; Heyd, J. J.; Brothers, K. . K. N.; Staroverov, V. N.; Kobayashi, R.; Normand, J.; Raghavachari, M. . R. Rendell, A.; Burant, J. C.; Iyengar, S. S.; Tomasi, J.; Cossi, V. . N.; Millam, N. J.; Klene, M.; Knox, J. E.; Cross, J. B.; Bakken, O. . Adamo, C.; Jaramillo, J.; Gomperts, R.; Stratmann, R. E.; Yazyev, R. L. . Austin, A. J.; Cammi, R.; Pomelli, C.; Ochterski, J. W.; Martin, P. . Morokuma, K.; Zakrzewski, V. G.; Voth, G. A.; Salvador, O. . Dannenberg, J. J.; Dapprich, S.; Daniels, A. D.; Farkas and D. J. Foresman, J. B.; Ortiz, J. V.; Cioslowski, J.; Fox, *Gaussian09, Revision C.01*, Gaussian, .
- 48 A. D. Becke, *Can. J. Chem.*, 1996, **74**, 995–997.
- 49 J. P. Perdew, *Phys. Rev. B*, 1986, **33**, 8822–8824.
- 50 J. P. Perdew, M. Ernzerhof and K. Burke, *Phys. Rev. Lett.*, 1996, **77**, 3865–3868.
- 51 S. Tao, J. P. Perdew, V. N. Staroverov and G. E. Scuseria, *Phys. Rev. Lett.*, 2003, **91**, 14601–14611.
- 52 Y. Zhao and D. G. Truhlar, *J. Chem. Phys.*, 2006, **125**, 194101-194118.
- 53 M. Ernzerhof and G. E. Scuseria, *J. Chem. Phys.*, 1999, **110**, 5029–5036.
- 54 Y. Zhao and D. G. Truhlar, *J. Phys. Chem. A*, 2004, **108**, 6908–6918.
- 55 M. Dolg, W. Küchle, H. Stoll and H. Preuss, *Mol. Phys.*, 1991, **74**, 1265–1285.
- 56 W. J. Hehre, R. Ditchfield and J. A. Pople, *J. Chem. Phys.*, 1972, **56**, 2257–2261.
- 57 S. Grimme, *J. Comput. Chem.*, 2004, **25**, 1463–1473.
- 58 S. I. Gorelsky and B. . Lever, *J. Organomet. Chem.*, 2001, **635**, 187–196.

- 59 D. Andrae, U. H. M. Dolg, H. Stoll and H. Preub, *Theor. Chim. Acta*, 1990, 123–141.
- 60 C. Samojłowicz, M. Bieniek and K. Grela, *Chem. Rev.*, 2009, **109**, 3708–3742.
- 61 A. Michrowska, R. Bujok, S. Harutyunyan, V. Sashuk, G. Dolgonos and K. Grela, *J. Am. Chem. Soc.*, 2004, **126**, 9318–9325.
- 62 A. Szadkowska, A. Makal, K. Woz, R. Kadyrov and K. Grela, *Organometallics*, 2009, 2693–2700.
- 63 D. J. Heisterberg, 1990. The Quatfit program, the CCL archive, 1990
- 64 C. a Jiménez-Hoyos, B. G. Janesko and G. E. Scuseria, *J. Phys. Chem. A*, 2009, **113**, 11742–11749.
- 65 Y. Minenkov, G. Occhipinti and V. R. Jensen, *J. Phys. Chem. A*, 2009, **113**, 11833–11844.
- 66 P. Śliwa and J. Handzlik, *Chem. Phys. Lett.*, 2010, **493**, 273–278.
- 67 K. Getty, M. U. Delgado-Jaime and P. Kennepohl, *J. Am. Chem. Soc.*, 2007, **129**, 15774–15776.
- 68 K. Paredes-Gil and P. Jaque, *Chem. Phys. Lett.*, 2015, **608**, 174–181.
- 69 P. Pérez, L. R. Domingo, A. Aizman and R. Contreras, *The electrophilicity index in organic chemistry in: Theoretical Aspects of Chemical Reactivity*, Elsevier, 2007, vol. 19.
- 70 K. Paredes-Gil, X. Solans-Monfort, L. Rodriguez-Santiago, M. Sodupe and P. Jaque, *Organometallics*, 2014, **33**, 6065–6075.
- 71 S. V. Vummaleti, L. Cavallo and A. Poater, *Theor. Chem. Acc.*, 2015, **134**, 22–28.
- 72 Y. Minenkov, G. Occhipinti and V. R. Jensen, *Organometallics*, 2013, **32**, 2099–2111.
- 73 O. Eisenstein, R. Hoffmann and A. R. Rossi, *J. Am. Chem. Soc.*, 1981, **103**, 5582–5584.

Table of contents

	Pag.
1. Colour Graphic	2
2. Text	3

## 1. Colour Graphic



## 2. Text

Reorganization energy and DFT-based reactivity descriptors revealed important issues on the performance of Grubbs catalysts.